On the Solid State Structure of 4-Iodobenzoic Acid

Cara L. Nygren,[†] Chick C. Wilson,[‡] and John F. C. Turner*[,§]

Department of Chemistry, University of Tennessee, Knoxville, Tennessee 37996-1600, Department of Chemistry, University of Glasgow, Glasgow, G12 8QQ United Kingdom, and Neutron Sciences Consortium and Department of Chemistry, University of Tennessee, Knoxville, Tennessee 37996-1600

Received: June 28, 2004; In Final Form: November 11, 2004

The solid-state structure of 4-iodobenzoic acid has been confirmed by variable temperature X-ray diffraction, variable temperature solid-state NMR and differential scanning calorimetry. 4-iodobenzoic acid crystallizes in the space group $P2_1/n$, and dimerizes in the solid state about a center of inversion. Using extensive X-ray crystallographic data collections, the placement of the carboxylate H atoms from the residual electron density in difference Fourier maps was determined. The position of the electron density associated with the proton is found to vary with temperature in that the population of the disordered sites changes with varying temperature. Determination of the crystal structure between the temperatures of 248 and 198 K was not possible due to a phase transition, an endothermic event occurring at 230.77 K. The phase transition is also indicated by a change in the relaxation time of the ring carbon atoms in the solid-state NMR data. Though the dominating force in the dimeric unit in the solid state is the presence of strong hydrogen bonds, there are also van der Waals forces present between the iodine atoms. In the layered structure, the iodine−iodine distance is within the van der Waals contact radii, an interaction which causes a deformation in the electron density of the iodine atoms.

I. Introduction

The carboxylic acid moiety is an important structural feature that occurs frequently in crystal engineering and biology.[1−4] In general, structures of carboxylic acids in the solid state are dominated by dimers in which the carbonyl oxygen and hydroxyl groups act as donors and acceptors.[2,5−35] The structure of this hydrogen-bonded dimer is shown in Figure 1.

As also shown in Figure 1, the full, real space hydrogen bond scheme is often developed via a crystallographic center of inversion.[5−16] However, the presence of a carboxylic acid group does not always imply the presence of a dimeric structure[36] and two-dimensional networks and chains have also been observed. In systems where the dimeric structure is observed, the degenerate nature of the atoms involved in the hydrogen-bonded carboxylic acid dimer has attracted the interest of the theoretical community as a model for proton transfer.[3,37−46]

The 4-halo benzoic acids crystallize isostructurally in the monoclinic space group $P2_1/n$[29,31−35,47,48] and are dimeric in the solid state, a phenomenon that is also persistent in solution.[49] The structure of 4-iodobenzoic acid has been known since 1982, when the powder diffraction pattern was first reported.[31] A single crystal diffraction experiment two years later also substantially confirmed the molecular structure and lattice.[29] In this paper, we examine the structure of 4-iodobenzoic acid to characterize the intermolecular hydrogen bond and to investigate the other forces that determine the structure of this material, employing a series of X-ray diffraction measurements, solid-state NMR, and differential scanning calorimetry in addition to spherical atom refinements of the diffraction data.

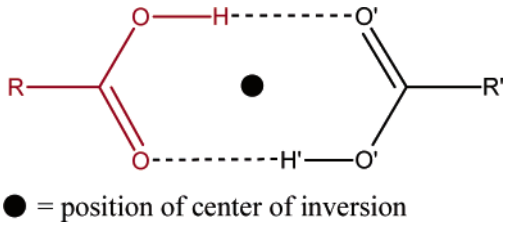

Figure 1. Schematic representation of a typical carboxylic acid dimer with the crystallographically generated atoms as X′.

4-Iodobenzoic acid is of interest as the molecular structure ensures that there are several possible identifiable forces that may exist in the lattice; the most obvious of these is the hydrogen-bonding interaction, but "π-stacking", van der Waals, dispersion, and multipole forces may all play a role. As we shall show, the structure that is evolved on crystallization is dependent on several of these factors, and we offer a qualitative ordering of the strength of these interactions; moreover, the presence of these forces is confirmed by the unsatisfactory spherical atom refinement of the diffraction data at any temperature. Given our interest in the structural chemistry of the hydrogen atom, we were interested in the arrangement of the hydrogen atom positions in the presence of a range of other possible interactions.

It is well accepted that the most common diffraction technique for the location of H atoms in a hydrogen bond is neutron diffraction. However, an important distinction must be made, in that a neutron diffraction experiment simply describes the nuclear density in the hydrogen bond and the distribution of electron density in a molecular system is only measurable by X-ray diffraction experiments. In many heavy atom systems, the nuclear and electron densities are strongly correlated; however, the density in a hydrogen bond is not correlated in the same manner.[50] The distribution of density in a 3-centered−4-electron bond such as the hydrogen bond is often diffuse and

[†] Department of Chemistry, University of Tennessee.
[‡] University of Glasgow.
[§] Neutron Sciences Consortium and Department of Chemistry, University of Tennessee.

10.1021/jp047189b CCC: $30.25
Published on Web 02/25/2005

TABLE 1: Selected Refinement Parameters for the Collected Data

T (K)	103	123	148	173
θ range (deg)	2.70−28.33	1.35−28.28	2.69−28.20	2.70−28.24
index range for data collection	$-5 \le h \le 5$	$-5 \le h \le 5$	$-5 \le h \le 5$	$-5 \le h \le 5$
	$-7 \le k \le 7$	$-7 \le k \le 7$	$-7 \le k \le 7$	$-7 \le k \le 7$
	$-39 \le l \le 39$	$-39 \le l \le 40$	$-40 \le l \le 40$	$-39 \le l \le 39$
no. of reflns collected	6519	6704	6783	7365
no. of ind reflns	1759	1755	1748	1781
	[R(int) = 0.0232]	[R(int) = 0.0267]	[R(int) = 0.0294]	[R(int) = 0.0267]
completeness to $\theta = 28.33°$	96.30%	96.00%	95.70%	97.20%
data/restraints/parameters	1759/0/93	1755/0/92	1748/0/92	1781/0/92
S	1.311	1.446	1.426	1.323
final R indices [$I > 2s(I)$]	$R1 = 0.0335$,	$R1 = 0.0574$,	$R1 = 0.0613$,	$R1 = 0.0423$,
	$wR2 = 0.0777$	$wR2 = 0.1492$	$wR2 = 0.1533$	$wR2 = 0.1011$
R indices (all data)	$R1 = 0.0366$,	$R1 = 0.0584$,	$R1 = 0.0627$,	$R1 = 0.0474$,
	$wR2 = 0.0785$	$wR2 = 0.1495$	$wR2 = 0.1538$	$wR2 = 0.1025$
T (K)	198	248	298	
θ range (deg)	1.35−28.25	2.70−28.29	1.36−28.24	
index range for data collection	$-5 \le h \le 5$	$-5 \le h \le 5$	$-5 \le h \le 5$	
	$-7 \le k \le 7$	$-8 \le k \le 8$	$-7 \le k \le 8$	
	$-39 \le l \le 39$	$-39 \le l \le 39$	$-39 \le l \le 39$	
no. of reflns collected	7325	7007	6917	
no. of ind reflns	1775	1789	1785	
	[R(int) = 0.0291]	[R(int) = 0.0283]	[R(int) = 0.0312	
completeness to $\theta = 28.33°$	96.20%	95.90%	96.10%	
data/restraints/parameters	1775/0/92	1789/0/92	1785/0/92	
S	1.319	1.358	1.308	
final R indices [$I > 2s(I)$]	$R1 = 0.0550$,	$R1 = 0.0417$,	$R1 = 0.0506$,	
	$wR2 = 0.1275$	$wR2 = 0.1047$	$wR2 = 0.1234$	
R indices (all data)	$R1 = 0.0607$,	$R1 = 0.0457$,	$R1 = 0.0589$,	
	$wR2 = 0.1292$	$wR2 = 0.1059$	$wR2 = 0.1260$	

anisotropic in nature; however, the nuclear density is generally not diffuse in a 3c−4e bond. Therefore, the only way to clearly demonstrate the distribution of electron density in a bond is through a series of extensive X-ray diffraction experiments.

II. Experimental Section

4-Iodobenzoic acid was purchased from Acros and was recrystallized from acetone. The material crystallizes as thin plates from the slow evaporation of an acetone solution (0.0534 M). For the temperature range 103−198 K, the crystals were mounted in a loop in Paratone oil. For temperatures of 223 K to room temperature, the crystals were mounted with epoxy on a glass fiber. Single-crystal X-ray diffraction data were collected using a Bruker AXS Smart 1000 diffractometer equipped with a CCD area detector and graphite monochromatized Mo source (Mo Kα, 0.71073 Å) and a Nicolet LT-2 cooling system. The crystal-to-detector distance was 5.0 cm. The parameters of each data collection are collated in Table 1.

More than a hemisphere of data were collected over the angular range of $2.70 < 2\theta < 28.33$ (103 K).[51] Frame widths of 0.3° were used for the data collection of 6519 reflections, counting 40 s per frame. Data reduction and spherical atom analyses were carried out using the Bruker program Saint[52] and the General Structure Analysis System (GSAS).[53] The unit cell dimensions were refined on the basis of 5544 reflections. A multiscan absorption correction was made using SADABS.[54] The data collection for 173 and 298 K was repeated and an analytical absorption correction[55] was used to ensure the results of the preceding experiments were valid, considering the habit of the crystal as well as the presence of iodine in the molecular structure. The results from these experiments showed little change in the hydrogen bond motif or in the residual electron density distributed around the iodine.

Systematic absences were consistent with the space group $P2_1/n$. A total of 6159 reflections were collected, and merging of equivalent reflections gave 1759 unique reflections (R_{int} = 2.32%), with 1622 classed as observed ($|F_o| > 4\sigma_F$). The structure was solved by direct methods (SHELXTL),[56] refined by the full matrix least-squares method, and completed by a series of difference Fourier syntheses. All non-hydrogen atoms were refined anisotropically, with the aromatic hydrogen atoms being introduced at idealized positions and refined using a riding model. Weighted R-factors, wR^2, and all goodness-of-fit values are based on F^2.

Differential scanning calorimetry was used to determine the thermodynamics of any phase behavior, using a Mettler Toledo DSC 820 with a temperature range of −120 to +100 °C and a heating/cooling rate of 10 °C/min. The samples were prepared in aluminum pans. For the measurement of heat capacity, the basic lines of the empty pan and sapphire reference were measured and compared to the heat flow measurements of the sample. The heat capacity of the sample was measured in two runs.

CPMAS solid-state NMR data were collected at a frequency of 100.550 MHz using a Varian INOVA 400 NMR spectrometer. The 90° pulse of proton resonance was 4 μs, the contact time was 5 ms and a MAS rate 6.555 kHz was used. A total of 400 transients were collected with a relaxation delay of 3 s and an acquisition time of 45 ms.

Solution NMR data were obtained using a Varian Mercury 300 MHz spectrometer, at which field the resonant frequency of ^{13}C is 75.454 MHz, with the ^{1}H frequency being 300.088 MHz, from solutions of the recrystallized material in DMSO-d_6. Chemical shifts were referenced to tetramethylsilane via residual ^{1}H residues in the solvent or the ^{13}C shift of the solvent.

III. Results

A. Temperature Variation and Structure of the Lattice. Diffraction data were collected from crystalline specimens of 4-iodobenzoic acid, grown from evaporation of an acetone solution, at temperatures of 103, 123, 148, 173, 198, 248, and 298 K. Initial spherical atom refinements were unsurprising and confirmed the previously determined space group of $P2_1/n$, and the room temperature lattice parameters were found to be similar

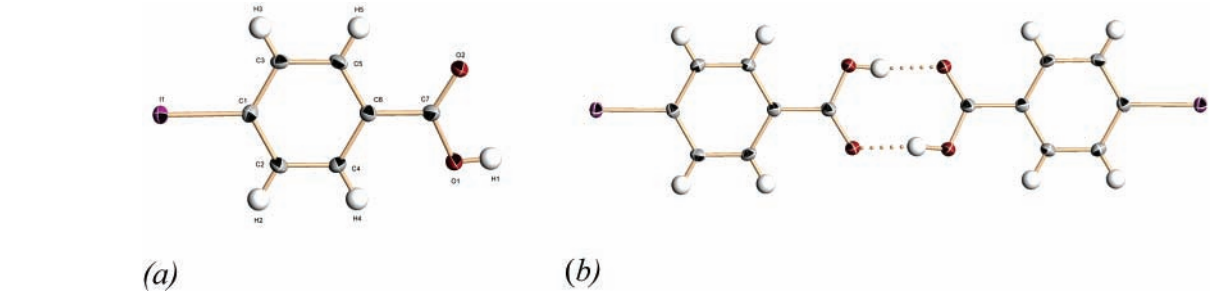

Figure 2. (a) Molecular structure of 4-iodobenzoic acid, corresponding to the asymmetric unit in the crystal, together with (b) the structure of the dimmer at 103K.

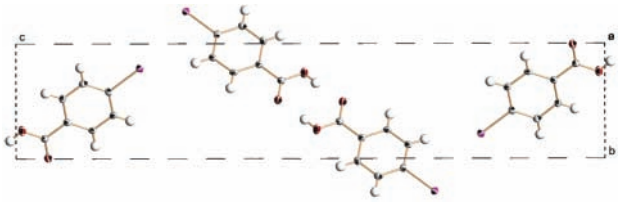

Figure 3. Packing diagram at 103 K showing the dimeric unit within the unit cell.

to the previously reported values.[29,31] The two sets of previously determined lattice constants are compiled in Table 2, together with the same constants determined in these experiments.

TABLE 2: Lattice Parameters (Reduced Unit Cell) for the Collected Data at Variable Temperature

a (Å)	*b* (Å)	*c* (Å)	β (deg)	*T* (K)	ref
4.160	6.040	30.108	90.48	298	31
4.156	6.030	30.109	90.52	298	29
4.0567(12)	5.9409(17)	30.223(9)	91.019(4)	103	this work
4.0688(10)	5.9466(15)	30.253(8)	90.982(4)	123	this work
4.0778(11)	5.9724(17)	30.243(8)	90.893(4)	148	this work
4.0960(13)	5.9745(19)	30.157(10)	90.852(5)	173	this work
4.1049(6)	5.9933(9)	30.179(5)	90.878(2)	198	this work
4.1305(5)	6.0075(7)	30.143(3)	90.731(2)	248	this work
4.1527(19)	6.009(3)	30.037(3	90.623(7)	298	this work

B. Molecular Structure from Spherical Atom Refinements. The gross molecular structure, determined from spherical atom refinements, is unsurprising with the non-hydrogenous structure remaining relatively invariant with temperature. A representative structure of the asymmetric unit is shown in Figure 2a together with the structure of the dimer evolved through the center of inversion. Figure 3 shows the unit cell for the lowest experimental temperature, and Figure 4 shows the asymmetric unit at the highest and lowest temperatures of measurement. Salient bond molecular structural parameters are given in Table 3, together with the labeling scheme.

TABLE 3: Selected Intramolecular Structural Parameters at Variable Temperature

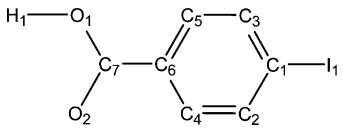

T (K)	$r_{O_1C_7}$ (Å)	$r_{O_2C_7}$ (Å)
103	1.300(7)	1.233(7)
123	1.295(13)	1.240(13)
148	1.284(13)	1.248(13)
173	1.281(8)	1.242(8)
198	1.282(11)	1.241(11)
248	1.277(8)	1.241(8)
298	1.268(10)	1.234(10)

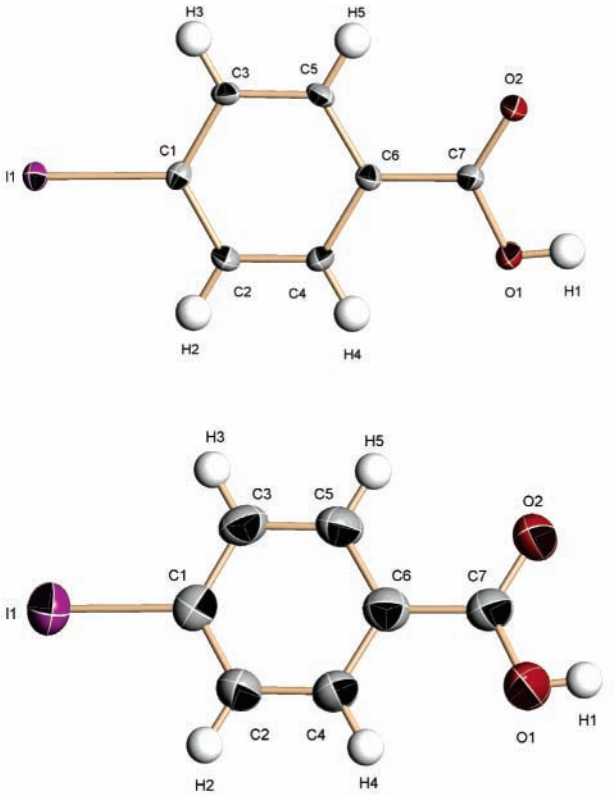

Figure 4. Representation of the asymmetric unit at 103 K (top) and 298 K (bottom).

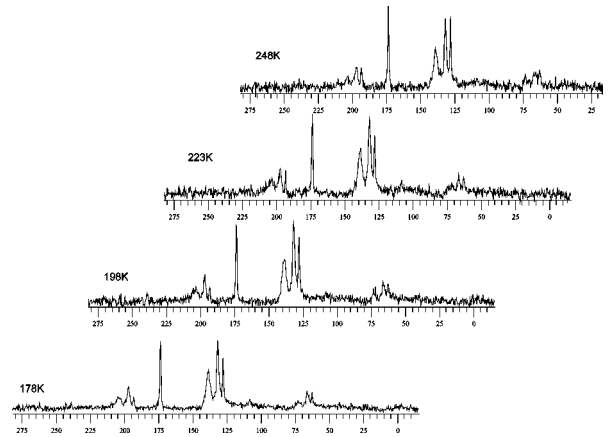

Figure 5. ^{13}C CPMAS SSNMR variable temperature spectra.

Solid-state NMR spectra were consistent with the asymmetric unit and are shown in Figure 5. These spectra also showed a slight change in the relaxation time for the ring carbon atoms, as determined from Lorentzian fits to the measured spectra. The resonances at δ/ppm = 138.94, δ/ppm = 131.80 and δ/ppm =

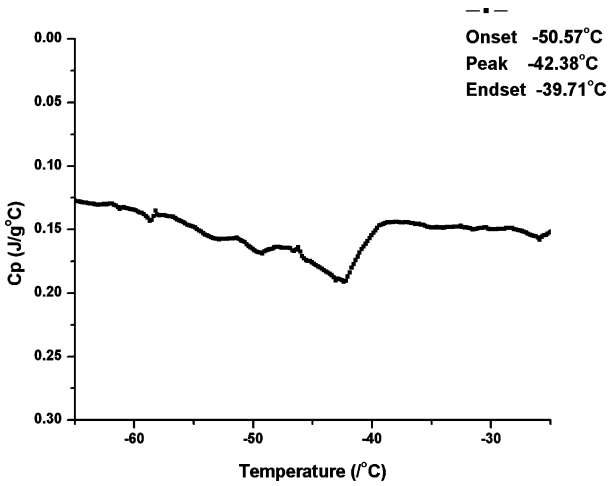

Figure 6. DSC data for 4-iodobenzoic acid, with the temperature transition centered around 230−233 K.

127.86 are assigned to the ring carbons (C2/3, C4/5 and C6 respectively), with the carboxylate carbon, C7, resonating at δ/ppm = 173.48.

Differential scanning calorimetry showed a small and broad endothermic event centered around 230.77 K; the onset of this transition is at 222.58 K and the transition is complete by 233.44 K. The temperature profile of the transition is shown in Figure 6 and the transition is characterized by a change in entropy (ΔS = −0.393 J K^{-1} mol^{-1}) and a change in enthalpy (ΔH = −91.77 J mol^{-1}).

IV. Discussion

The intention of this study was to analyze and understand the electron density associated with the hydrogen atom involved in the hydrogen-bonded dimer interaction and follow these changes with temperature. Diffraction data collected at variable temperature revealed the expected intramolecular structure with apparently little change in this structure with temperature. However, repeated attempts at structure solution from the 223 K data set were unsuccessful. Data were re-collected at 223 K several times, each time the reflections could not be indexed. When the data were indexed using a known unit cell from the 198 K data collection, the agreement in the reflections was poor. Of 800 reflections analyzed using Smart,[51] all 800 were indexed in *h* and *k*, but only 205 were indexed in *l*. The final structure solution from this attempt led to unreliable results with *R*-factors of greater than 35% when using the atomic positions and thermal parameters from the 198 K data set. The putative molecular structure from this attempted refinement was unphysical with respect to geometry, bond lengths, and angles. Differential scanning calorimetry in the temperature range 153−373 K revealed a broad phase transition centered at 230 K. Analysis of the relaxation times of the ^{13}C resonances of the 4-iodobenzoic acid also showed a change in T_2 at the transition temperature for the phase transition. This phase transition does not, however, cause any drastic change in the molecular structure. The ^{13}C isotropic chemical shift in the solid state ($\Delta\delta$ = 29.293 Hz) show little variation, though static wide line spectra were not recorded and so no determination of the individual components of the chemical shift anisotropy are therefore given.

That the phase change is minor is clear from the magnitude of the thermodynamic parameters. The change in entropy and enthalpy determined from the two DSC experiments are ΔS = −0.393 J K^{-1} mol^{-1} and ΔH = −91.77 J mol^{-1}, respectively. The differences observed in the two sets of data are due to the residual solvent present in the first run that was subsequently evaporated upon heating of the sample.

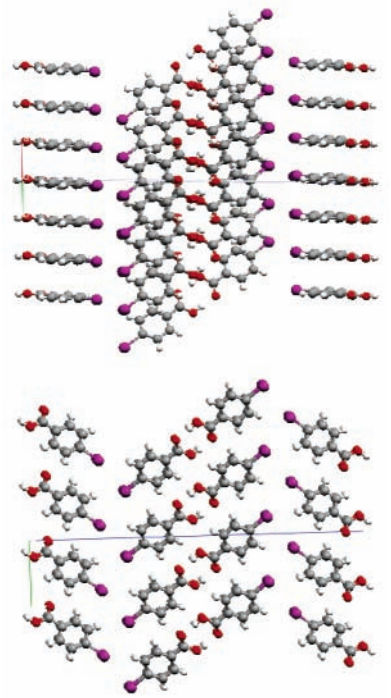

Figure 7. Packing diagrams from the 103 K data set demonstrating the stacking of the dimeric units as well as the I−I interactions.

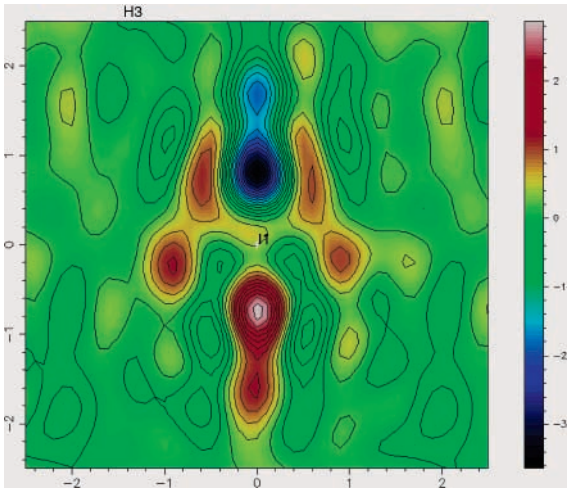

Figure 8. Fourier difference map showing the residual electron density around the iodine position at 103 K ranging from −3.64 to +2.87 e$^-$/Å^3.

In common with many carboxylic acids, the dimeric unit present in 4-iodobenzoic acid is generated by the presence of a center of inversion and this center of inversion lies in the plane of the carboxylate group. Figure 4 shows the two asymmetric units for the low and high temperature phases. Unsurprisingly, these dimeric units persist at all temperatures of measurement, with the only observable structural difference between them being the hydrogen positions, vide infra. As such, the description of the crystal is best discussed using the dimer as the basic chemical unit present.

This dimeric unit is stacked in single stacks and a series of packing diagrams are presented in Figure 7, showing the arrangement of the dimers. Interestingly, the dimeric units are arranged in the maximum energy configuration with respect to the dipole moment present on each acid moiety, though the net dipole moment of the dimer is clearly zero.

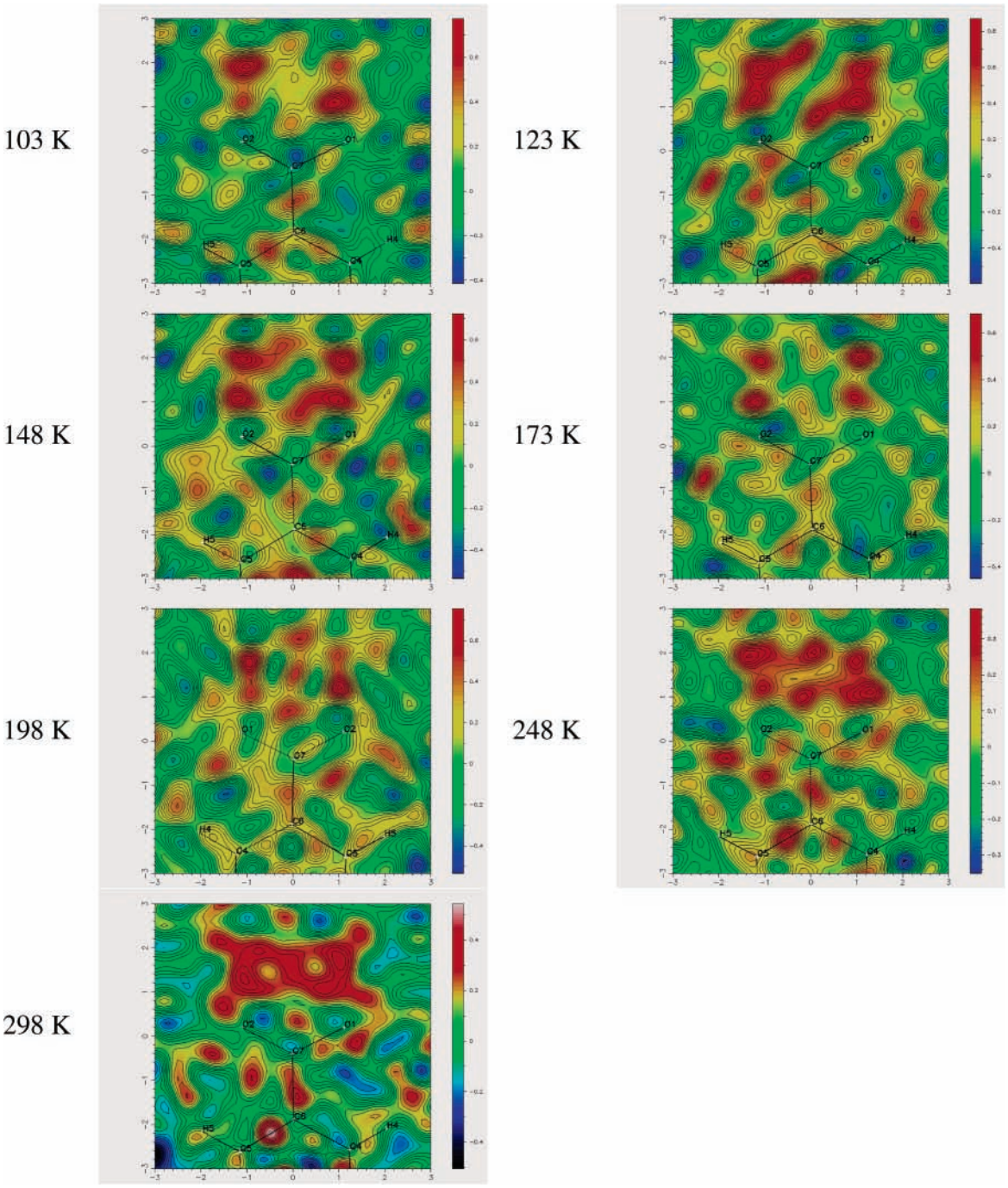

Figure 9. Fourier difference maps showing the carboxylate proton position in the dimeric unit from the spherical atom refinement.[60] Contour levels are drawn at 0.04 e Å^{-3}.

These one-dimensional lamellæ are bound through interactions between the iodine atoms. This interaction is strong and is the dominant structure-developing force in the crystal, after the hydrogen bond interaction. The interaction between iodine atoms occurs both between molecules in the layers and between iodine atoms of adjacent layers. The interlayer iodine−iodine contact distance ranges from 4.075 to 4.153 Å for the available temperature range of experimental data. The van der Waals radius for I is 1.98 Å,[57] which implies that there is a nonbonding contact between the iodine atoms. However, the iodine−iodine distance between adjacent layers ranges from 3.932 to 3.992 Å for the given temperature range, distances that are within the van der Waals radius sum for two iodine atoms.

The strength of the I−I interaction is seen in the spherical atom refinements carried out; the electron density at each I atom is highly distorted and cannot be adequately described by a spherical atom model. The residual electron density surrounding the iodine atom ranges from −4.24 to +2.84 e Å^{-3} when an empirical absorption correction was applied for the 173 K data set.[54] When an analytical absorption correction was applied to a data set at the same temperature, the residual electron density ranges from −5.78 to +2.05 e Å^{-3}.[56] Figure 8 shows a difference Fourier map of the distribution of the residual electron density around the I atom following an empirical absorption correction at 103 K. The deformation of this electron density protrudes perpendicular to the plane of the asymmetric unit. This raises questions as to the driving force for the packing. Though hydrogen bonding is an obvious driving force for the formation of the dimeric unit, the iodine−iodine contacts appear to be the interactions that drive the disposition of the lamellar

TABLE 4: Population of the Major (A) Configuration in the Structure of 4-Iodobenzoic Acid

T (K)	$X_{A,F}$	$1 - X_{A,F}$	$K_{H,F}$	ln $K_{H,F}$	$X_{A,SOF}$	$1 - X_{A,SOF}$	$K_{H,SOF}$	ln $K_{H,SOF}$	ITF
103	0.578	0.422	1.37	0.314	0.6779	0.3221	2.105	0.744	0.029
123	0.525	0.475	1.10	0.099	0.6201	0.3799	1.6323	0.490	0.022
148	0.491	0.509	0.96	−0.037	0.6861	0.3139	2.1857	0.782	0.028
173	0.457	0.543	0.84	−0.171	0.6146	0.3854	1.5947	0.467	0.028
198	0.412	0.588	0.70	−0.355	0.638	0.362	1.7624	0.567	0.052
248[b]	*0.547*	*0.453*	*1.21*	*0.190*	*0.5502*	*0.4498*	*1.2232*	*0.201*	*0.037*
298[b]	*0.503*	*0.497*	*1.01*	*0.012*	*0.633*	*0.376*	*1.6835*	*0.521*	*0.034*

[a] The linear region is in the low-temperature range, up to 198 K. The SOF, site occupancy factor, refinements are less reliable for these split site H atoms than are the occupancies estimated from direct imaging from the Fourier maps.[61] [X_A is the population of the major configuration as determined from examination of the difference Fourier maps. $K = (X_A)/(1 - X_A)$. ITF is the isotropic thermal factor.] [b] These data above the phase transition were excluded from the thermodynamic fit.

structure. In a search of the Cambridge Structural Database (CSD), this type of halogen−halogen interaction is found to be quite common for 1,4-substituted benzene molecules, with the shortest reported contact distance for the I−I contact being 3.748 Å.[58,59]

In terms of the intramolecular structure of 4-iodobenzoic acid, all bond lengths and angles are well within the normal observed range.[58,59] The torsion angles described by O1−C7 and C6−C4 [6.6(8)°] and by O2−C7 and C6−C5 [6.8(8)°] are typical for benzoic acid derivatives. The oxygen−carbon−oxygen angle of the carboxylate unit has a value of 123.2(5)°, which is typical of carboxylic acid units. A search of the CSD demonstrates that the range for the O−C−O angle in 4-substituted benzoic acid molecules is 113.6−128.4°.[58,59]

The dimeric unit is held together by the presence of a strong hydrogen bond. The electron density associated with the H atom in this bond was located in Fourier difference maps, $\rho_{diff,1} = F_{obs} - F_{calc}$, with no placement of the H atom in the calculated model. Fourier maps at successive temperatures are shown in Figure 9. Table 4 shows the site occupancy factors for each temperature for the distribution of electron density associated with the H atom position and the 3-center−4-electron (3c−4e) bond between dimers.

As seen in the difference Fourier maps in Figure 9, at 103 K the electron density associated with the hydrogen-bonded proton position (H1) is strongly associated with only one of the oxygen atoms in the carboxylic acid unit.[60] However, this correlation changes dramatically with temperature, in accord with previous studies in similar systems.[61] In the 173 K data, for example, there appears to be a "split-site" disorder associated with the electron density in the hydrogen bond. This trend is followed with increasing temperature, but at room temperature, the presence of thermal motion and disorder does not allow us to image adequately the distribution of the electron density associated with the hydrogen atom in the hydrogen bond.

It is reasonable to assume that the observed peaks in the Fourier maps are due to a disordered population over two possible H atom sites. A valence bond representation of the two possible forms **I** and **II** observed in the average structure is shown in Figure 10, illustrating the hydrogen bond split-site equilibrium. Moreover, it is assumed that there is no order in the distribution of these valence bond representations from unit cell to unit cell and that therefore the distribution is statistically random. No evidence of any ordering of the dimeric units with respect to **I** and **II** or any resulting superlattice was found in the diffraction data; we note that if the only discrimination between a system of valence bond isomers ordered over a superlattice and a randomly disordered situation were the location of the hydrogen atoms, then these X-ray diffraction experiments would be unlikely to reveal them, given the scattering power of the electron density associated with a hydrogen atom.

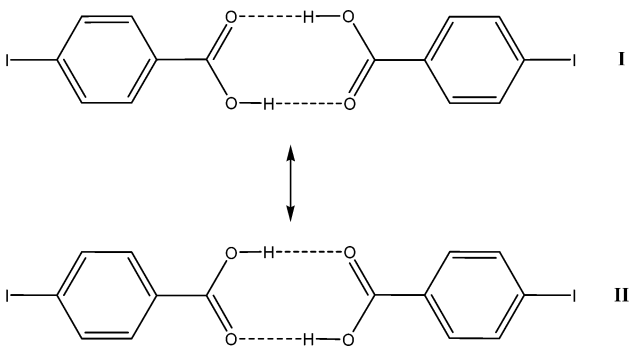

I **II**

Figure 10. Valence bond representations of the split-site equilibrium in 4-iodobenzoic acid.

Taking a perfectly disordered system, as described above, as the model for the data, then an equilibrium constant, K_H, can be written as

$$K_H = \frac{X_A}{X_B} = \frac{X_A}{(1 - X_A)}$$

assuming a site occupancy over the disordered hydrogen atom sites such that

$$X_A + X_B = 1$$

where X_i is the population of the ith atom site.

Using the definition of K_H, it follows that

$$\ln K_H = \frac{-\Delta G}{RT} = \frac{-\Delta H}{RT} + \frac{\Delta S}{R} \qquad \text{at any temperature } T$$

ΔG is the difference in Gibbs free energy for the two isomers with populations A and B. Table 4 contains the results of the population analyses derived from the integration of the Fourier map, with a data cutoff of $F_{obs}/\sigma(F_{obs}) = 0$ and the site occupancy factors, SOF, from the spherical atom refinements of the data. A plot of ln $K_{H,(Fourier)}$ vs inverse temperature for temperatures in the range 103−198 K is shown in Figure 11. From the slope of the linear fit to the data, $\Delta H/R = 135.43$, yielding a value for ΔH of 1.13 kJ mol^{-1} for the enthalpy difference between the configurations. This value compares favorably with other similar measurements, viz. 0.50(4) kJ mol^{-1} for benzoic acid[62,63] and 1.64(9) kJ mol^{-1} for *p*-chlorobenzoic acid[64] obtained previously from neutron diffraction data.

Interestingly, despite the clearly strong trend in the redistribution of proton occupancies between the two oxygen atoms in the COOH unit, there is no parallel trend evident in the C−O bond length differences; the simple **I**/**II** site model does not reproduce the bond lengths observed in this study. Indeed, inspection of the CSD for carboxylic acid dimers and extracting the O−H, C−O, and C═O bond lengths reveals that there is

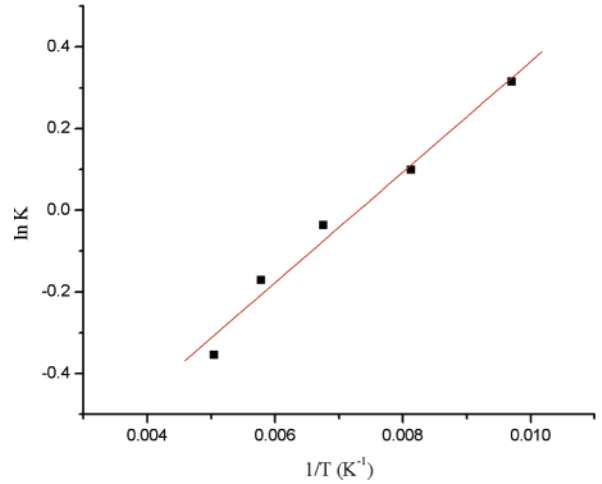

Figure 11. Plot of ln K_H, vs inverse temperature for the split-site populations, extracted from the integration of the Fourier map with a data cutoff of $F_{obs}/\sigma(F) = 0$. As $\Delta H/R = 135.44$, $\Delta H = 1.126$ kJ mol^{-1} for the enthalpy difference between the sites.

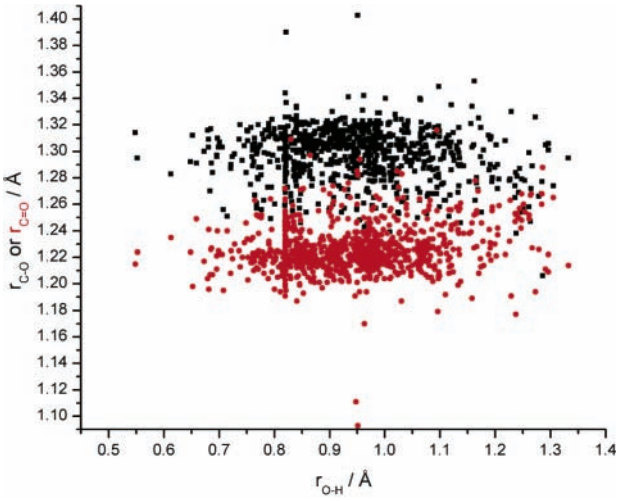

Figure 12. Comparison of the O−H vs C−O and O−H vs C═O (red) distances, r_{O-H}, r_{C-O}, and $r_{C=O}$, extracted from the CCSD, showing no correlation between these structural parameters.

no correlation between these structural parameters; the accumulated data are shown in Figure 12.

The lack of correlation between these parameters implies that the simple **I/II** model is not supported by the data; if the **I/II** model were to apply, a bimodal distribution would be expected. Moreover, an average bond length determined by r_{C-O} and $r_{C=O}$ and weighted to the hydrogen atom populations does not account for the observed variation of these carbon−oxygen bonds with temperature in this study.

Clearly, there is complex relationship between the H atom distributions and the structural response of the [CO_2] unit which is not adequately described by the **I/II** model. We note that theoretical descriptions of hydrogen bonding show that the rearrangement of the total electron distribution in the system must be considered, not simply that local to the COOH unit. These fine details of the bonding picture are, however, inaccessible from this study. It is also clear that the carboxylate moiety is not the only important interaction in the system. The I−I interactions between adjacent molecules and between lamellæ are also very strong and determine the packing of dimers in the system

V. Conclusions

This study, by determining the electron density associated with the hydrogen atom participating in an apparently well-understood structural moiety, has shown that a simple delocalized approach to the determination of the hydrogen atom disorder is not as complete as might be desired. A split-site model of the distribution of the electron density directly associated with the hydrogen atom, obtained from difference Fourier maps yield values for the enthalpy differences between the two distinct molecular configurations in the lattice that are consistent with previous measurements. However, the structural consequences of this model for the carboxylate group in terms of a valence bond delocalized picture of the bonding are not fully borne out in the observed C···O bond lengths determined from spherical atom refinements of the data, suggesting further complexity. The application of theoretical calculations to this and similar systems, as well as charge density analysis, are in progress.

Acknowledgment. J.F.C.T. acknowledges the financial support of the University of Tennessee, through provision of start-up funds, and the Petroleum Research Fund, administered through the American Chemical Society (PRF-37341-G4). C.C.W. acknowledges this work was funded in part by EPSRC under grant number GR/R04690.

Supporting Information Available: Variable temperature X-ray diffraction data are available free of charge via the Internet at http://pubs.acs.org

References and Notes

(1) Sekiya, R.; Nishikiori, S.-I. *Chem.—Eur. J.* **2002**, *8*, 4803−4810.
(2) Smith, G.; White, J. M. *Aust. J. Chem.* **2001**, *54*, 97−100.
(3) Foces-Foces, C.; Echevarria, A.; Jagerovic, N.; Alkorta, I.; Elguero, J.; Langer, U.; Klein, O.; Minguet-Bonvehi, M.; Limbach, H.-H. *J. Am. Chem. Soc.* **2001**, *123*, 7898−7906.
(4) Ashton, P. R.; Fyfe, M. C. T.; Hickingbottom, S. K.; Menzer, S.; Stoddart, J. F.; White, A. J. P.; Williams, D. J. *Chem.—Eur. J.* **1998**, *4*, 577−589.
(5) Papadakis, M. M.; Martins, S. P.; Thompson, H. W.; Lalancette, R. A. *Acta Crystallogr., Sect. C: Cryst. Struct. Commun.* **2002**, *C58*, o321−o322.
(6) Luner, P. E.; Patel, A. D.; Swenson, D. C. *Acta Crystallogr., Sect. C: Cryst. Struct. Commun.* **2002**, *C58*, o333−o335.
(7) Gilardi, R.; Butcher, R. J.; Bashir-Hashemi, A. *Acta Crystallogr., Sect. E: Struct. Rep. Online* **2002**, *E58*, o860−o861.
(8) Crispini, A.; Neve, F. *Acta Crystallogr., Sect. C: Cryst. Struct. Commun.* **2002**, *C58*, o34−o35.
(9) Hokelek, T.; Patir, S.; Ergun, Y.; Okay, G. *Acta Crystallogr., Sect. C: Cryst. Struct. Commun.* **2001**, *C57*, 414−416.
(10) Degen, A.; Bolte, M. *Acta Crystallogr., Sect. C: Cryst. Struct. Commun.* **1999**, *C55*, 1306−1308.
(11) Fitzgerald, L. J.; Gerkin, R. E. *Acta Crystallogr., Sect. C: Cryst. Struct. Commun.* **1998**, *C54*, 966−969.
(12) Dobson, A. J.; Gerkin, R. E. *Acta Crystallogr., Sect. C: Cryst. Struct. Commun.* **1998**, *C54*, 795−798.
(13) Fitzgerald, L. J.; Gerkin, R. E. *Acta Crystallogr., Sect. C: Cryst. Struct. Commun.* **1997**, *C53*, 1080−1082.
(14) Fitzgerald, L. J.; Gerkin, R. E. *Acta Crystallogr., Sect. C: Cryst. Struct. Commun.* **1997**, *C53*, 1265−1267.
(15) Ferguson, G.; Gallagher, J. F.; McAlees, A. J. *Acta Crystallogr., Sect. C: Cryst. Struct. Commun.* **1995**, *C51*, 454−458.
(16) Thompson, H. W.; Lalancette, R. A.; Vanderhoff, P. A. *Acta Crystallogr., Sect. C: Cryst. Struct. Commun.* **1992**, *C48*, 66−70.
(17) Kumar, V. S. S.; Nangia, A.; Katz, A. K.; Carrell, H. L. *Cryst. Growth Des.* **2002**, *2*, 313−318.
(18) Thalladi, V. R.; Nuesse, M.; Boese, R. *J. Am. Chem. Soc.* **2000**, *122*, 9227−9236.
(19) Kariuki, B. M.; Bauer, C. L.; Harris, K. D. M.; Teat, S. J. *Angew. Chem., Int. Ed.* **2000**, *39*, 4485−4488.
(20) Martin, S. B.; Valente, E. J. *J. Chem. Crystallogr.* **1998**, *28*, 203−207.

(21) Fitzgerald, L. J.; Gerkin, R. E. *Acta Crystallogr., Sect. C: Cryst. Struct. Commun.* **1997**, *C53*, 71−73.
(22) Blackburn, A. C.; Dobson, A. J.; Gerkin, R. E. *Acta Crystallogr., Sect. C: Cryst. Struct. Commun.* **1996**, *C52*, 907−910.
(23) Blackburn, A. C.; Dobson, A. J.; Gerkin, R. E. *Acta Crystallogr., Sect. C: Cryst. Struct. Commun.* **1996**, *C52*, 1482−1486.
(24) Blackburn, A. C.; Dobson, A. J.; Gerkin, R. E. *Acta Crystallogr., Sect. C: Cryst. Struct. Commun.* **1996**, *C52*, 1486-1488.
(25) Blackburn, A. C.; Dobson, A. J.; Gerkin, R. E. *Acta Crystallogr., Sect. C: Cryst. Struct. Commun.* **1996**, *C52*, 2320−2323.
(26) Blackburn, A. C.; Dobson, A. J.; Gerkin, R. E. *Acta Crystallogr., Sect. C: Cryst. Struct. Commun.* **1996**, *C52*, 2638−2641.
(27) Smith, G.; Lynch, D. E.; Byriel, K. A.; Kennard, C. H. L. *Aust. J. Chem.* **1995**, *48*, 1133−1149.
(28) Smith, G.; Lynch, D. E.; Byriel, K. A.; Kennard, C. H. L. *Acta Crystallogr., Sect. C: Cryst. Struct. Commun.* **1995**, *C51*, 2629−2633.
(29) Baughman, R. G.; Nelson, J. E. *Acta Crystallogr., Sect. C: Cryst. Struct. Commun.* **1984**, *C40*, 204−206.
(30) Lynch, D. E.; Smith, G.; Byriel, K. A.; Kennard, C. H. L. *Aust. J. Chem*, **1991**, *44*, 1017−1022.
(31) Takaki, Y.; Kurisu, A.; Nakata, K. *Bull. Chem. Soc. Jpn.* **1982**, *55*, 319−320.
(32) Ohkura, K.; Kashino, S.; Haisa, M. *Bull. Chem. Soc. Jpn.* **1972**, *45*, 2651−2652.
(33) Miller, R. S. *Organic gas−solid reactions and the single crystal X-ray structure of 4-chlorobenzoic acid*. Ph.D. Thesis, University Illinois, Urbana, IL, USA. FIELD URL, 1973; p 216.
(34) Miller, R. S.; Paul, I. C.; Curtin, D. Y. *J. Am. Chem. Soc.* **1974**, *96*, 6334−6339.
(35) Colapietro, M.; Domenicano, A.; Pela Ceccarini, G. *Acta Crystallogr., Sect. B: Struct. Crystallogr. Cryst. Chem.* **1979**, *B35*, 890−894.
(36) Butcher, R. J.; Bashir-Hashemi, A.; Gilardi, R. D. *J. Chem. Crystallogr.* **1997**, *27*, 99−107.
(37) Basilevsky, M. V.; Vener, M. V. *Russ. Chem. Rev.* **2003**, *72*, 1−33.
(38) Wilson, C. C. *New J. Chem.* **2002**, *26*, 1733−1739.
(39) Maurin, J. K.; Czarnocki, Z.; Wojtasiewicz, K.; Maleszewska, E.; Magdziak, K.; Paluchowska, B. *J. Mol. Struct.* **2002**, *610*, 33−40.
(40) Gavezzotti, A. *J. Mol. Struct.* **2002**, *615*, 5−12.
(41) Fillaux, F.; Limage, M. H.; Romain, F. *Chem. Phys.* **2002**, *276*, 181−210.
(42) Latanowicz, L.; Reynhardt, E. C. *Chem. Phys. Lett.* **2001**, *341*, 561−567.
(43) Fillaux, F. *Int. Rev. Phys. Chem.* **2000**, *19*, 553−564.
(44) Grabowski, S. J.; Krygowski, T. M. *Chem. Phys. Lett.* **1999**, *305*, 247−250.
(45) Loerting, T.; Liedl, K. R. *J. Am. Chem. Soc.* **1998**, *120*, 12595−12600.
(46) Horsewill, A. J.; Brougham, D. F.; Jenkinson, R. I.; McGloin, C. J.; Trommsdorff, H. P.; Johnson, M. R. *Ber. Bunsen-Ges.* **1998**, *102*, 317−324.
(47) Toussaint, J. *Acta Crystallogr.* **1951**, *4*, 71−72.
(48) Pollock, J. M.; Woodward, I. *Acta Crystallogr.* **1954**, *7*, 605.
(49) Hanrahan, E. S.; Bruce, B. D. *Spectrochim. Acta, Part A: Mol. Biomol. Spectrosc.* **1967**, *23*, 2497−2503.
(50) Nygren, C. L.; Wilson, C. C.; Schultz, A. J.; Piccoli, P. M. B.; Turner, J. F. C. *J. Phys. Chem.*, in press.
(51) *Smart*; Bruker AXS, Inc.: Madison, WI, 1997.
(52) *Saint*; Bruker AXS, Inc: Madison, WI, 1997.
(53) Larson, A. C.; Von Dreele, R. B. Report LAUR 86-748; Los Alamos National Laboratory, 2000.
(54) Sheldrick, G. M. *SADABS*; Univerisity of Gottingen: Gottingen, Germany, 1996.
(55) *XPREP*; Bruker AXS, Inc: Madison, WI, 1997.
(56) Sheldrick, G. M. *SHELXTL*; University of Gottingen: Gottingen, Germany, 1997.
(57) Winter, M. http://www.webelements.com/.
(58) Allen, F. H.; Motherwell, W. D. S. *Acta Crystallogr.* **2002**, *B58*, 407−422.
(59) Bruno, I. J.; Cole, J. C.; Edgington, P. R.; Kessler, M.; Macrae, C. F.; McCabe, P.; Pearson, J.; Taylor, R. *Acta Crystallogr.* **2002**, *B58*, 389−397.
(60) Farrugia, L. J. *J. Appl. Crystallogr.* **1999**, *32*, 837−838.
(61) Wilson, C. C.; Goeta, A. E. *Angew. Chem., Int. Ed.* **2004**, *43*, 2095−2099.
(62) Wilson, C. C.; Shankland, N.; Florence, A. J. *J. Chem. Soc., Faraday Trans.* **1996**, *92*, 5051−5057.
(63) Wilson, C. C.; Shankland, N.; Florence, A. J. *Chem. Phys. Lett.* **1996**, *253*, 103−107.
(64) Wilson, C. C.; Florence, A. J.; Xu, X.; Shankland, N. *New J. Chem.*, submitted for publication.